

Düzce University Journal of Science & Technology



https://dergipark.org.tr/tr/pub/dubited



Research paper

A Dual-Branch Shunt-Diode RF Rectifier with Wideband and Wide Dynamic Input Power Range for Wireless Power Transfer



^alğdır University, Vocational School of Technical Sciences, Department of Electricity and Energy, Iğdır, Türkiye.

^bIğdır University, Faculty of Engineering, Department of Electrical and Electronics Engineering, Iğdır, Türkiye.

cState University of New Paltz, School of Science and Engineering, Department of Electrical Engineering, New York, USA.

*Corresponding author: sadik.zuhur@igdir.edu.tr

Article information:

Received: 13/03/2025, Revision: 13/06/2025, Accepted: 29/06/2025

DOI: 10.29130/dubited.1657055

ABSTRACT

In this study, a dual-branch, dual-shunt-diode rectifier has been designed and its performance has been thoroughly analyzed for wideband RF energy harvesting applications. The proposed structure features a compact design with dimensions of 19 mm \times 21 mm, utilizing FR4 as the substrate. To reduce losses caused by built-in potential (V_{bi}) and breakdown voltage (V_{br}), a dual-branch design was implemented, with each branch incorporating shunt diodes as rectifiers. In addition to schematic simulations, electromagnetic simulations were conducted, demonstrating that the rectifier operates efficiently over a wide bandwidth and a broad input power range. According to simulation results, the proposed rectifier achieves a power conversion efficiency (PCE) exceeding 65% across the 1.6 – 3.4 GHz frequency range, with a peak PCE of 75.23% observed at 2 GHz under an input power of 10.8 dBm. Moreover, at 2 GHz, the rectifier maintains a PCE above 50% over a -1 to 13 dBm input power range. Compared to existing studies, the proposed rectifier stands out due to its wide bandwidth, broad input power range, high power conversion efficiency, and compact design. Therefore, this work presents an effective alternative for low-power autonomous devices.

Keywords: RF Energy Harvesting, Schottky Diode, Impedance Matching, FR4, Electromagnetic Simulation

I. INTRODUCTION

Research on wireless power transfer and RF energy harvesting has been gaining popularity as it supports the autonomous operation of low-power electronic devices. Current studies in this field focus on high-efficiency, low-loss rectifiers capable of harvesting energy over a wide frequency band and broad input power range (Argote-Aguilar et al., 2024; He and Liu, 2020; Muhammad et al., 2023; Zhang et al., 2024).

The main challenge in the design of these rectifiers is that the input impedance of the diode-coupled rectifier varies nonlinearly with frequency and input power, especially in wide-band applications (Halimi, 2024). To overcome this problem, researchers have proposed various advanced impedance matching techniques, such as multi-stage transmission lines (Wu et al., 2019), asymmetric capacitive structures (Cheng et al., 2024), and innovative self-impedance matching methods that enable compact designs without the need for a separate matching network (Gyawali et al., 2024).

In the literature, RF rectifier designs with an fractional bandwidth (FBW) greater than 20%, determined according to the -10 dB return loss (S11) criterion, are generally classified as wide-band (Joy et al., 2024). For example, (He & Liu, 2024) reported a 44.4% bandwidth in the 2.1 - 3.3 GHz range and a power conversion efficiency (PCE) of 70% at 14 dBm input power. Similarly, (Wu et al., 2019) presented an ultrawideband rectifier operating in the 2.0 - 3.05 GHz frequency range and achieved an efficiency of 70% at 10 dBm input power.

These studies highlight the critical role of wideband performance in environmental RF energy harvesting applications, as the frequency and polarization of environmental signals change. Therefore, optimizing impedance-matching networks and diode configurations is crucial for broadband rectifier design.

Microwave rectifier topologies can be classified as voltage doubler (Liu et al., 2020; Mansour & Kanaya, 2018), series diode (Lin et al., 2018), and shunt diode (Arpanutud et al., 2024; Hirakawa & Shinohara, 2021) configurations. The shunt diode topology is widely used in RF rectifier circuits.

The design of dual-band rectifiers aims to achieve high power conversion efficiency (PCE) at different frequencies. For example, a study by (Bui et al., 2023a) developed an inverse Class-F shunt diode rectifier operating at 2.4 GHz and 3.5 GHz. This design, which uses five transmission lines for harmonic optimization, achieved 64% efficiency at both frequencies. This harmonic optimization is based on the principle of controlling unwanted harmonic signals generated during rectification and shaping the voltage and current waveforms on the diode to maximize efficiency (Khodaei et al., 2024). For example, while Class-F designs terminate even harmonics with short circuits, Inverse Class-F adopts the opposite approach, and with these methods, it has been possible to achieve over 80% efficiency (Nguyen et al., 2023). However, the study by (Bui et al., 2023a) did not consider a wide-band harvesting approach and was limited to dual-band harvesting.

Another study (Bui et al., 2023b) emphasized that the harvesting performance of rectifiers is generally affected by diode losses and impedance mismatches. To reduce these losses, the study proposed parallel diode connections. The proposed single-band rectifier (915 MHz) was tested, and a PCE of 75.3% was achieved with a single-diode system and 78.3% with a dual-diode system. Simulations showed that the dynamic range of the single-diode circuit ranged from -9 dBm to 6.5 dBm, while the dual-diode circuit ranged from -10.5 dBm to 14 dBm. The same study emphasized that parallel diode connections effectively reduce diode-induced losses and impedance mismatches.

Another innovative approach to reducing diode losses is to apply a bias voltage to the rectifier from an external power source. In this context, a system has been developed that simultaneously harvests RF and ground energy and uses the latter to bias rectifier diodes (Shi et al., 2024). This method significantly increases rectification efficiency, especially at low RF input powers. Furthermore, 3D omnidirectional rectifier arrays capable of capturing all polarizations are being developed to efficiently collect RF signals with uncertain direction and polarization encountered in real-world applications (Jing et al., 2024).

In this study, a compact RF rectifier with dimensions of 19 mm \times 21 mm was designed and validated with electromagnetic simulations. To reduce power losses due to the internal potential voltage (V_{bi}) and breakdown voltage (V_{br}) of the rectifier elements, a double-branch topology consisting of two shunt-connected diodes was chosen instead of a single diode. This design approach reduces power losses by balancing the voltage stress on each diode. While many studies in the literature focus on wide-band operation or a wide input power range, the proposed rectifier demonstrates high performance in both areas. The proposed architecture achieves over 65% power conversion efficiency (PCE) at 10.8 dBm input power in the 1.6 to 3.4 GHz frequency band. It also achieves over 50% PCE at the 2 GHz center frequency over an input power range of -1 dBm to 13 dBm. These results demonstrate that the proposed architecture offers a robust and efficient RF energy harvesting solution for real-world applications with variable signal conditions.

II. DESIGN OF THE PROPOSED STRUCTURE

The schematic representation of the proposed structure is detailed in Figure 1(a). To facilitate analysis, a simplified schematic representation is provided in Figure 1(b). In Figure 1(a), HSMS 2860 diodes are used

as rectifiers, benefiting from their low threshold voltage. Capacitors C1 and C2 serve as DC blocks, preventing the DC components of the RF signal from passing to the rectifier section. Inductors L2 and L3 function as compensation elements, ensuring impedance matching in both branches. To filter the output voltage, inductor L3 and capacitor C3 are utilized, allowing the DC component to reach the resistive load (R). At the circuit input, an RF source with a 50 Ω impedance is placed, and the circuit is matched to this input impedance.

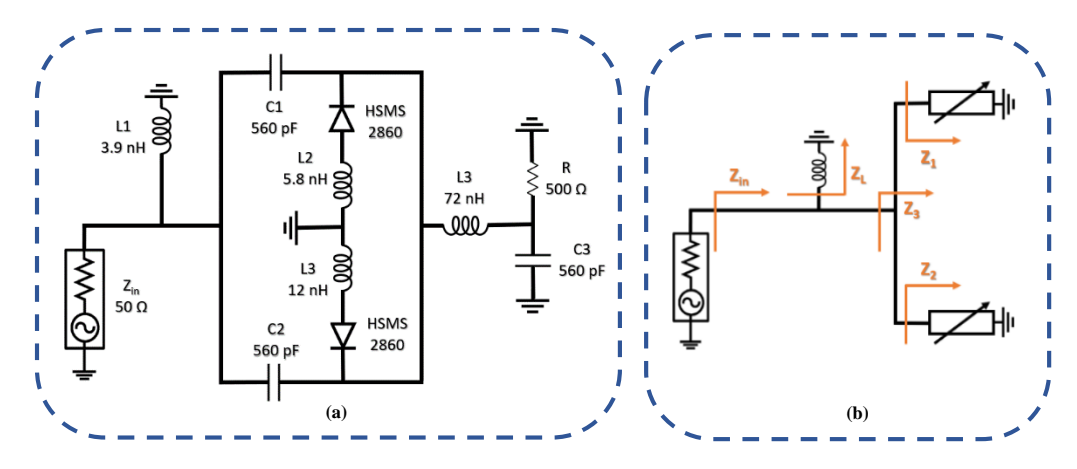


Figure 1. (a) Detailed schematic of the proposed rectifier circuit. (b) Equivalent block diagram used for input impedance analysis.

The design process was first initiated by determining a structure that could provide high rectification efficiency at low input powers. For this purpose, A double-branch topology with two shunt diodes was preferred over a single diode to reduce voltage losses across the diode. Then, L2 and L3 inductors were added to optimize the input impedance of each branch, and the effects of these inductors were analyzed separately. By connecting the two branches in parallel, the real part of the input impedance was brought closer to $50~\Omega$. However, a parallel L1 inductor was added to the system to balance the imaginary part of the impedance. In the final stage, microstrip lines were included in the circuit in order to achieve broadband impedance matching. Thus, wide-band matching was achieved between 1.6~-~3.4~ GHz. Thanks to this stepwise optimization approach, both impedance matching and rectifier efficiency were improved.

From the simplified representation (Figure 1(b)), the input impedance (Z_{in}) can be expressed in terms of Z_1 , Z_2 , and Z_L using Eq. 1:

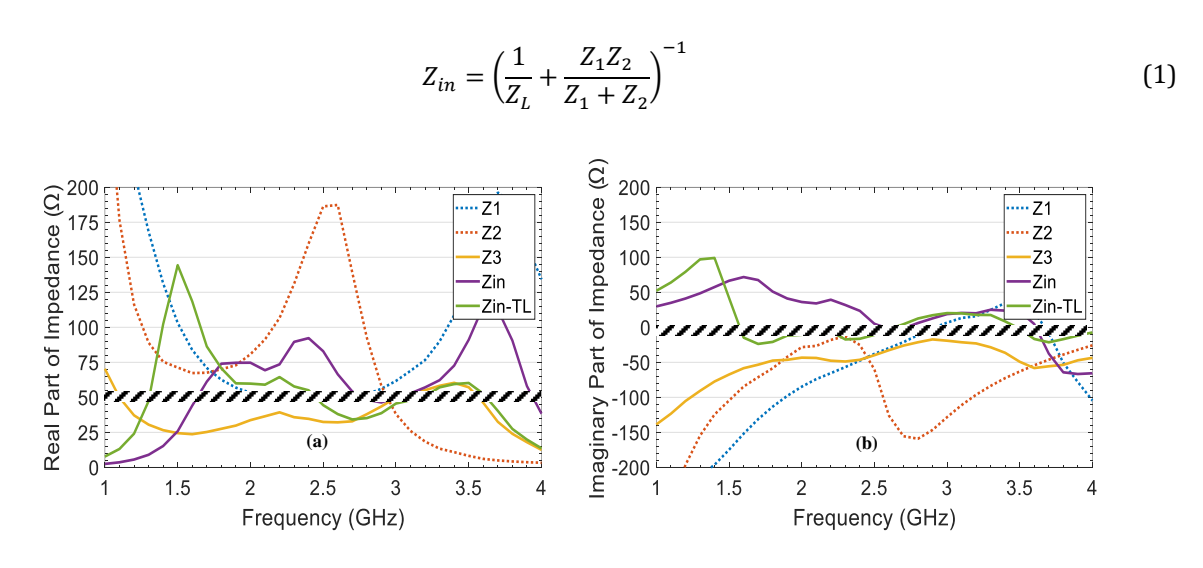


Figure 2. (a) Real and (b) imaginary parts of the input impedance for individual branches and the complete structure. The transition from Z_1/Z_2 to Z_3 and finally to Zin-TL illustrates the step-by-step matching improvement process.

In Figure 2, the input impedances of the first branch (Z_1) and the second branch (Z_2) are presented. The graphs indicate that with the addition and optimization of L2 and L3 inductors, impedance matching is achieved at specific frequencies. However, a wideband impedance match was not obtained.

To reduce losses, these two branches were connected in parallel, resulting in the Z_3 impedance graph. The Z_3 graph shows that the real part of the input impedance approaches 50 Ω (Figure 2(a)), while the imaginary part nears zero but still deviates from the optimal matching condition (Figure 2(b)). To further reduce the imaginary component of Z_3 , an additional parallel inductor (L1) was added and optimized, completing the impedance matching process and yielding the Zin graph. Finally, transmission lines were incorporated to finalize the matching process, resulting in the Z_{in} -TL graph, which demonstrates successful impedance matching across the 1.5 – 3.4 GHz frequency range.

III. SIMULATION RESULTS AND DISCUSSION

Power Conversion Efficiency (PCE) is a fundamental performance measure for RF rectifier circuits and is the ratio of the output DC power available at the load to the input RF power applied to the circuit. It is expressed as a percentage and is calculated using Eq. 2:

$$PCE = \frac{P_{out}}{P_{in}} \cdot 100\% = \frac{V_{out}^2}{R_L \cdot P_{in}} \cdot 100\%$$
 (2)

where, V_{out} represents the output voltage across the load resistor R_L , and P_{in} and P_{out} represent the input and output power of the circuit. This equation provides a quantitative assessment of how efficiently the rectifier converts incoming RF energy to DC power. A higher PCE value indicates a more efficient design for energy harvesting applications.

In this study, the design process was carried out using Keysight Advanced Design System (ADS) 2020 software. The design was targeted for the 1 GHz – 4 GHz frequency band at an input power of 10 dBm, with a 500 Ω load. The objective was to achieve the maximum output voltage, and performance evaluation was conducted based on PCE using Eq. 2.

The proposed structure was schematically tested using Large Signal S-Parameter Harmonic Balance and Harmonic Balance simulators. Subsequently, it was subjected to Momentum simulation in Microwave mode. The proposed rectifier was designed on an FR4 substrate (ϵ_r =4.6, $\tan(\delta)$ =0.01, thickness = 1.6 mm) using Avago HSMS-2860 Schottky diodes. Figure 1(a) previously illustrated the schematic representation of the rectifier.

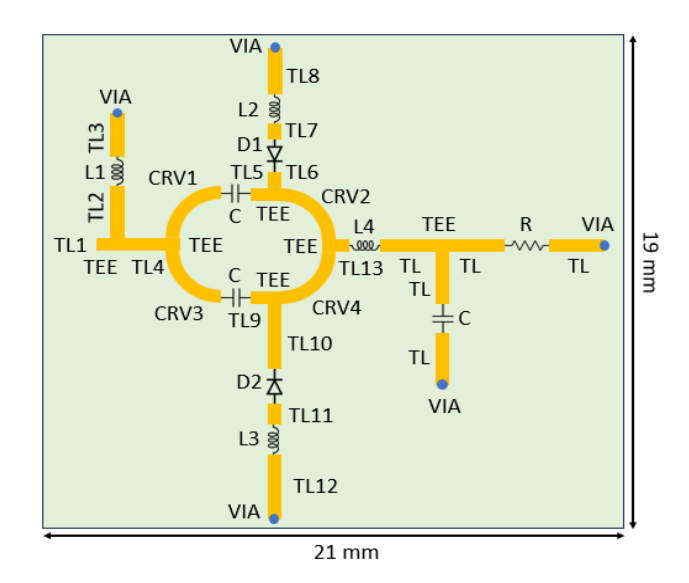


Figure 3. Layout of the Proposed Structure

In Figure 3, the layout of the design is presented. The proposed rectifier has a compact design with dimensions of 19 mm \times 21 mm. In the simulations, Murata brand LQW15AN3N9B00 (L1, 3.9 nH), LQW15AN5N8B00 (L2, 5.8 nH), LQW15AN12NG00 (L3, 12 nH), and LQW18AN72NG00 (L4, 72 nH) inductors, as well as the GCM1555C1H561FA16 (C, 560 pF) capacitor model, were used. Additionally, the Kamaya RGC116S-4990F (R, 499 Ω) resistor model was utilized. Moreover, Table 1 provides the dimensions of the optimized transmission lines used in the design.

Table 1. Dimensions of the	e Optimized Transr	nission Lines in the Desi	ign

Transmission Line	Length (mm)	Transmission Line	Length (mm)			
TL1	. ,	TL9	0.59			
117	0.5	1 L9	0.59			
TL2	2	TL10	2.5			
TL3	1.72	TL11	0.84			
TL4	1.54	TL12	2.5			
TL5	0.59	TL13	0.5			
TL6	0.5	TEE	0.53			
TL7	0.57	TL	2			
TL8	1.88 All widths are 0.53 mm					
CRV1,2,3,4 Radius=2.5 mm Angle=90°						

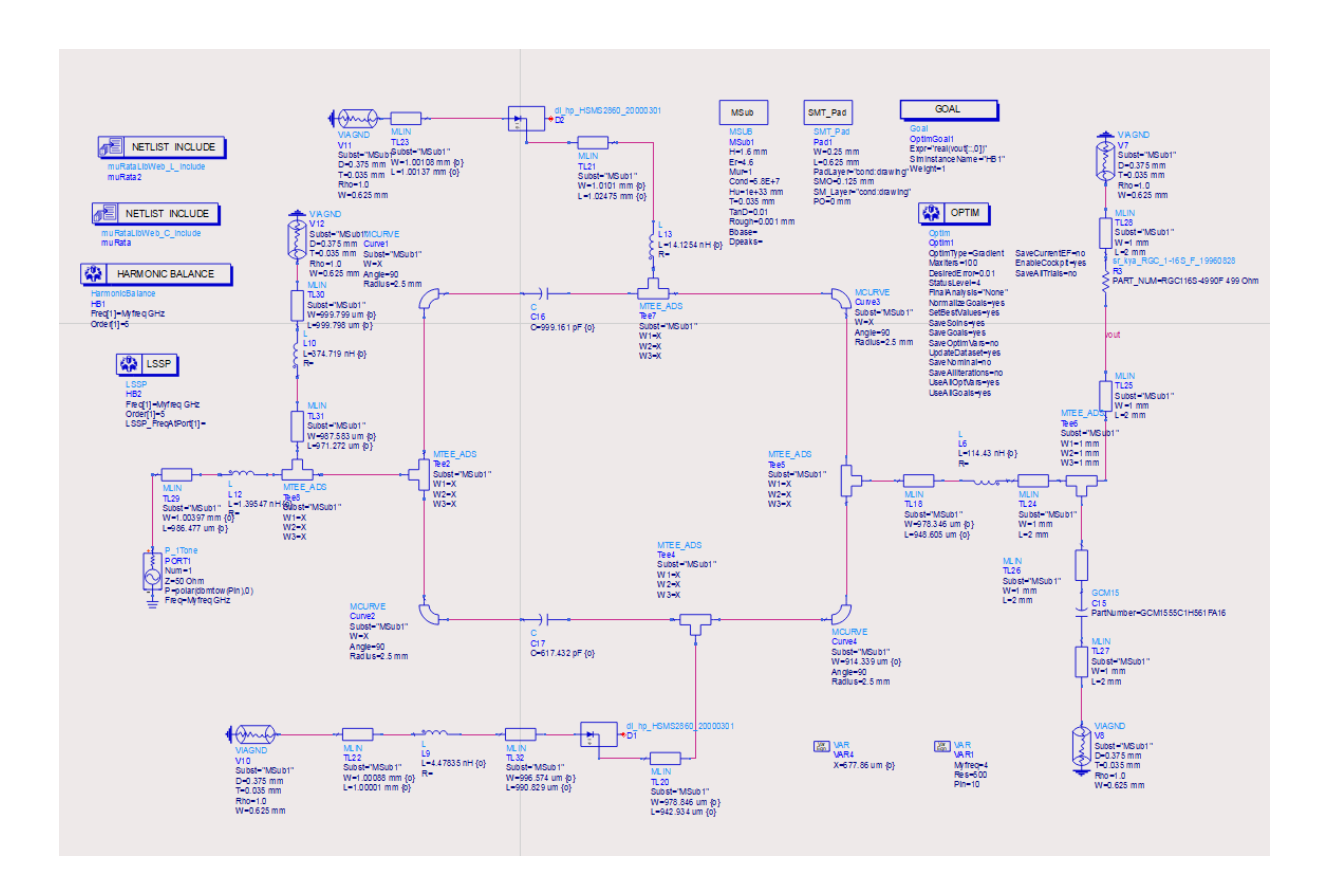


Figure 4. Simulation setup in ADS, including input source and matching network.

To enhance the repeatability of the simulations and offer a detailed technical framework, the simulation settings are described below. In the analyses performed at the schematic level, the impedance matching was optimized using the Harmonic Balance (HB) and Large Signal S-Parameter methods and the PCE was evaluated. In this context, "schematic" refers to circuit-level simulations based on component models, which do not include physical layout effects or electromagnetic coupling. For electromagnetic verification, the design was analyzed with the Momentum EM simulator in Microwave mode. Frequency scanning was performed between 1 GHz and 4 GHz with a 10 MHz step interval; the input power was varied between -20

dBm and +20 dBm. A 499 Ω resistive load was used at the output. All passive circuit elements were selected from real SMD models to ensure suitability for practical application. Figure 4 illustrates the simulation setup, including input sources and matching components. The consistency between the schematic- and EM-level simulation results in terms of S11 and Vout confirms the validity of the design methodology and enhances its reproducibility.

In Figure 5, the reflection coefficient (S11) and PCE graphs at an input power of $10.8~\mathrm{dBm}$ are presented. These results confirm that the rectifier achieves efficient impedance matching and energy conversion over a wide frequency range, which supports the wideband performance capability of the proposed design. The EM and schematic simulation results show strong agreement, as illustrated in the graphs. According to the EM simulation results, the reflection coefficient drops below -10 dB in the $1.5-3.4~\mathrm{GHz}$ range, which corresponds to a PCE exceeding 65% within this range. Another noteworthy point is the minimal fluctuation in PCE, with the maximum PCE of 75.23% observed at 2 GHz. To justify the use of the term "wideband," the fractional bandwidth (FBW) is calculated using the Eq. 3:

$$FBW = \frac{f_{high} - f_{low}}{f_{center}} \times 100 \tag{3}$$

where f_{high} = 3.4 GHz, f_{low} = 1.6 GHz, and f_{center} = 2.5 GHz. This yields a fractional bandwidth of approximately 77.5%, which justifies the wideband classification of the proposed design.

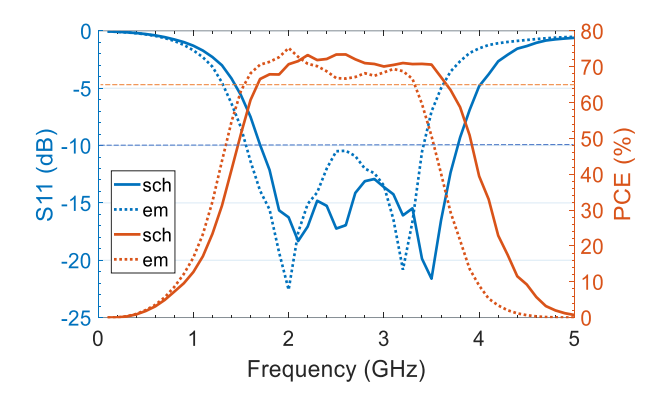


Figure 5. Reflection Coefficient and Power Conversion Efficiency at 10.8 dBm Input Power

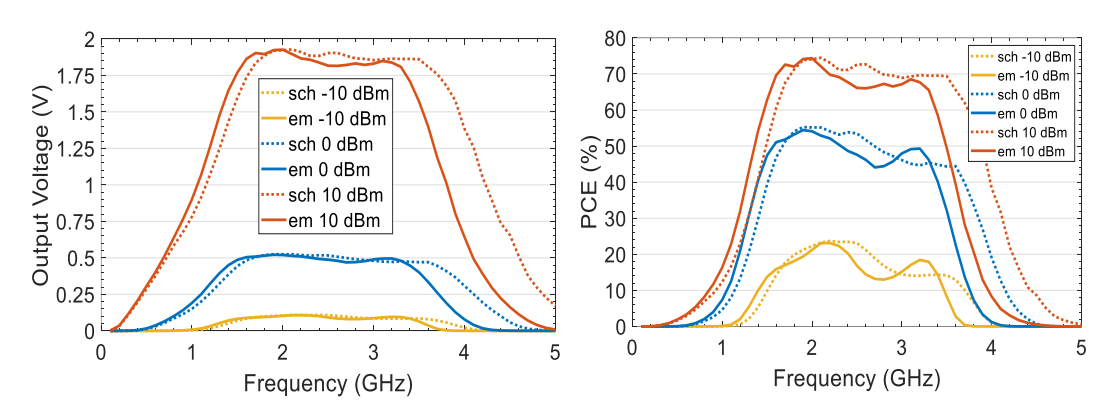


Figure 6. Output Voltage (a) and Power Conversion Efficiency (b) at Different Input Power Levels and Frequencies

In Figure 6(a) and 6(b), the schematic and EM simulation results for output voltage and PCE at input power levels of -10 dBm, 0 dBm, and 10 dBm are compared. This comparison demonstrates the circuit's ability to maintain stable output and acceptable efficiency across varying power levels, confirming its suitability for fluctuating RF environments. It is important that the rectifier exhibits stable performance

bands across different power levels. According to the EM simulation results, in the 1.4 – 3.4 GHz frequency range, the PCE exceeds 10% at -10 dBm input power and 40% at 0 dBm input power (Figure 5(b)). Within this range, the output voltage remains above 70 mV at -10 dBm and above 450 mV at 0 dBm (Figure 5(a)). At -10 dBm input power, the maximum PCE was determined as 23.1% at 2.2 GHz, while at 0 dBm input power, the maximum PCE reached 54.4% at 1.9 GHz. For the 10 dBm design input power, the PCE exceeded 65% in the 1.6 – 3.3 GHz frequency range, while the output voltage remained above 1.8 V within the same range. Additionally, at 10 dBm input power, a PCE above 70% was achieved within the 1.6 – 2.2 GHz frequency range.

In Figure 7, the output voltage and PCE at 2 GHz frequency for different input power levels are presented. The consistency of PCE above 50% within the -1 dBm to 13 dBm range emphasizes the dynamic range capability of the design, which is a key parameter in real-world wireless power applications. When Figure 5 and Figure 6 are evaluated together, it is evident that the proposed rectifier operates efficiently over both a wide frequency band range and a broad input power range.

Finally, according to the performance comparison with existing studies presented in Table 2, the proposed rectifier stands out due to its wide frequency range, broad input power range, compact design, and the use of an inexpensive substrate such as FR4 in the design. Although some previous studies report higher peak PCE values, these designs usually have disadvantages such as limited bandwidth, narrow input power range, or large circuit size. For example, although the study [3] provides a wide frequency range, it occupies a relatively large area of $70 \times 70 \text{ mm}^2$. However, the study [23] provides high PCE only in a narrow range and requires an expensive substrate such as Taconic TLY-5. In contrast, the proposed design offers a high efficiency of 75.23% at 2 GHz, operates effectively in the frequency range of 1.5–3.4 GHz and input power range of -1 to 13 dBm, and achieves this with standard, low-cost PCB technology. These combined features demonstrate that the proposed rectifier provides an application-oriented, scalable, and cost-effective solution.

Table 2. Dimensions of the Optimized Transmission Lines in the Design

Ref	Year	Bandwidth (GHz) PCE>%60	Dynamic Range (dBm) PCE>%50	Max. PCE	Size mm ²	Substrate	Diode Type
(Nguyen & Seo, 2022)	2022	1.6 - 2.8 @10 dBm	3 -16* @2.5 GHz	%81 @1.8 GHz* @ 12 dBm	32×46	Taconic TLY-5	HSMS2860
(Muhammad et al., 2023)	2023	1.8 - 3.2 @9.5 dBm	-9 - 5* @1.8 GHz	%77 @1.8 GHz @ 3 dBm	70×70	RO4003C	HSMS2850
(Liu et al., 2024)	2024	1.9 - 3.1 @0 dBm	-8 - 5* 2.4 GHz	%79.6 2.9 GHz 4 dBm	20×23	NA	HSMS 2860
(Wang et al., 2025)	2025	1.4 - 2.5 @18 dBm	-5 - 13 @1.6 GHz	72.5 @1.6 GHz @8 dBm	16×18	RO4003C	HSMS2852
This Work	2025	1.5 - 3.4 @10.8 dBm	-1 - 13 @2 GHz	%75 @2 GHz @10.8 dBm	19×21	FR4	HSMS2860

^{*}Graphically estimated NA is Not Available

In this study, FR4 is preferred as the substrate material due to its low cost and widespread availability in standard printed circuit board (PCB) manufacturing processes. Although FR4 has a relatively high dielectric loss factor (tan $\delta \approx 0.01$), it offers a sufficient balance between performance and cost. If a low-loss substrate such as Rogers RO3003, RO3004 or RT/duroid series were used improvement in impedance matching, reduction in reflection losses and increase in PCE values could be expected, especially at high frequencies. However, such materials significantly increase the production cost and are not suitable for large-scale or cost-sensitive applications. Therefore, the use of FR4 in the proposed design was preferred as a practical and economical solution.

IV. CONCLUSION

In this study, a double-branch shunt-diode rectifier structure was designed and thoroughly analyzed for wideband RF energy harvesting and wireless power transfer applications. Compared to other studies in the literature, the proposed rectifier achieved high efficiency over a wide bandwidth, providing a PCE above 65% in the 1.6 – 3.4 GHz frequency range at 10.8 dBm input power. Additionally, a PCE of over 50% was achieved at 2 GHz over an input power range of -1 dBm to 13 dBm.

The results show that both EM and schematic simulations are in strong agreement. Shunt diodes connected to both branches and an optimized impedance matching network effectively minimized losses, increasing the rectifier's PCE. Furthermore, the use of an FR4 substrate in the compact rectifier design provides cost advantages for practical applications.

Compared to recent studies in the literature, this study stands out with its high PCE across a wide frequency band, wide input power range, and compact design. Furthermore, the proposed rectifier design can be easily fabricated using standard PCB processes. The circuit utilizes standard and commercially available components such as Murata inductors and Kamaya resistors. The FR4 substrate, the preferred material in the design, is a widely used and low-cost material in the industry. Thanks to its compact dimensions (19 mm \times 21 mm) and layout verified by EM simulations, the circuit can be easily fabricated using standard printed circuit board (PCB) fabrication processes without requiring any specialized equipment.

Thanks to its wide frequency band and wide input power range, the proposed rectifier circuit is well-suited for a variety of low-power, autonomous applications. These applications include IoT-based sensor nodes, wireless medical monitoring devices, wearable electronics, environmental monitoring platforms, and remote data collection systems. The design's compact and low-cost structure also makes it an attractive option for large-scale applications such as smart agriculture, industrial monitoring, and smart infrastructure systems. Future work could explore different diode types and substrate materials to further enhance the design's performance.

DECLARATIONS

Acknowledgements: The author/authors do not wish to acknowledge any individual or institution.

Author Contributions: Conceptualization, S.Z.; Methodology, S.Z.; Validation, S.Z.; Investigation, S.Z.; Resources, S.Z.; Data Curation, S.Z.; Writing—Original Draft, S.Z.; Writing—Review & Editing, M.S.B; Supervision, M.S.B.. All authors have read and approved the final version of manuscript.

Conflict of Interest Disclosure: The authors declare no conflict of interest.

Copyright Statement: The authors retain the copyright of their work published in the journal, which is licensed under the CC BY-NC 4.0 license, allowing others to share and adapt the work for non-commercial purposes with appropriate attribution.

Funding/Supporting Organizations: This research received no external funding.

Ethical Approval and Participant Consent: This study does not involve human or animal participants. All procedures followed scientific and ethical principles, and all referenced studies are appropriately cited.

Availability of Data and Materials: Data sharing is applicable to this study.

Plagiarism Statement: This article has been evaluated for plagiarism and no instances of plagiarism were detected.

Use of AI Tools: OpenAI ChatGPT-5 were used in the language and readability adjustments of this study.

REFERENCES

- Argote-Aguilar, J., Wei, M., Hutu, F., Villemaud, G., Gautier, M., & Berder, O. (2024). Wide power range RF energy harvester for powering ultralow-power devices. *IEEE Transactions on Microwave Theory and Techniques*, 72(10), 5632–5642. https://doi.org/10.1109/TMTT.2024.3397389
- Arpanutud, K., Pongthavornkamol, T., Akkaraekthalin, P., & Chalermwisutkul, S. (2024). Design and optimization of single-shunt diode RF rectifier using electromagnetic co-simulation. In *Proceedings* 12th International Electrical Engineering Congress: Smart Factory and Intelligent Technology for Tomorrow (iEECON 2024) (pp. 1–4). https://doi.org/10.1109/iEECON60677.2024.10537951
- Bui, G. T., Nguyen, D. A., & Seo, C. (2023a). A novel design of dual-band inverse class-F shunt-diode rectifier for energy harvesting. *IEEE Transactions on Circuits and Systems II: Express Briefs, 70*(7), 2345–2349. https://doi.org/10.1109/TCSII.2023.3240501
- Bui, G. T., Nguyen, D. A., & Seo, C. (2023b). A novel methodology to improve efficiency and extend dynamic range of shunt-diode class-F rectifier for wireless power transfer. *IEEE Access*, *11*, 126643–126649. https://doi.org/10.1109/ACCESS.2023.3331757
- Cheng, F., Du, C. H., Wu, L., & Gu, C. (2024). Compact and ultra-wideband high-efficiency rectifier using asymmetric coupled-line impedance transformer. *International Journal of Microwave and Wireless Technologies*, 1–6. https://doi.org/10.1017/S1759078724000813
- Gyawali, B., Aboualalaa, M., Barakat, A., & Pokharel, R. K. (2024). Design of miniaturized Sub-6 GHz rectifier with self-impedance matching technique. *IEEE Transactions on Circuits and Systems I: Regular Papers*, 71(7), 3413–3422. https://doi.org/10.1109/TCSI.2024.3397810
- Halimi, M. A. (2024). A broadband rectifier with high power conversion efficiency and high power handling capability for microwave power transfer applications. In *Proceedings of the 2024 IEEE Wireless Antennas and Microwave Symposium (WAMS)* (pp. 1–4). https://doi.org/10.1109/WAMS59642.2024.10527855
- He, Z., & Liu, C. (2020). A compact high-efficiency broadband rectifier with a wide dynamic range of input power for energy harvesting. *IEEE Microwave and Wireless Components Letters*, 30(4), 433–436. https://doi.org/10.1109/LMWC.2020.2979711
- Hirakawa, T., & Shinohara, N. (2021). Theoretical analysis and novel simulation for single shunt rectifiers. *IEEE Access*, *9*, 16615–16622. https://doi.org/10.1109/ACCESS.2021.3053251
- Jing, J., Yan, L., & Liu, C. (2024). All-polarized wideband rectenna array for omnidirectional wireless energy harvesting. In *2024 IEEE Wireless Power Technology Conference and Expo (WPTCE)* (pp. 429–432). https://doi.org/10.1109/WPTCE59894.2024.10557393
- Joy, J. A., Palaniswamy, S. K., Kumar, S., Kanagasabai, M., Choi, H. C., & Kim, K. W. (2024). Thirty two port super wideband diversity antenna for indoor communications. *Scientific Reports, 14*(1), Article 25104. https://doi.org/10.1038/s41598-024-76008-6
- Khodaei, M., Boutayeb, H., & Talbi, L. (2024). A high efficiency and ultra-wideband rectenna for RF energy harvesting application. In *2024 18th European Conference on Antennas and Propagation (EuCAP)* (pp. 1–4). https://doi.org/10.23919/EuCAP60739.2024.10501246
- Lin, Y. L., Zhang, X. Y., Du, Z. X., & Lin, Q. W. (2018). High-efficiency microwave rectifier with extended operating bandwidth. *IEEE Transactions on Circuits and Systems II: Express Briefs*, 65(7), 819–823. https://doi.org/10.1109/TCSII.2017.2716538
- Liu, W., Huang, K., Wang, T., Zhang, Z., & Hou, J. (2020). A broadband high-efficiency RF rectifier for ambient RF energy harvesting. *IEEE Microwave and Wireless Components Letters, 30*(12), 1185–1188. https://doi.org/10.1109/LMWC.2020.3028607
- Liu, Y., Liu, W., Yin, D., Wang, T., Huang, X., & Qin, J. (2024). A compact broadband RF rectifier using two-stage microstrip lines. *Microwave and Optical Technology Letters*, 66(6), 1–6. https://doi.org/10.1002/mop.34225
- Mansour, M. M., & Kanaya, H. (2018). Compact and broadband RF rectifier with 1.5 octave bandwidth based on a simple pair of L-section matching network. *IEEE Microwave and Wireless Components Letters,* 28(4), 335–337. https://doi.org/10.1109/LMWC.2018.2808419
- Muhammad, S., Waly, M. I., Mallat, N. K., AlJarallah, N. A., Ghayoula, R., Negm, A. S., Smida, A., & Iqbal, A. (2023). Wideband RF rectifier circuit for low-powered IoT wireless sensor nodes. *AEU International Journal of Electronics and Communications*, 170, Article 154787. https://doi.org/10.1016/j.aeue.2023.154787
- Nguyen, D. A., & Seo, C. (2022). Design of high-efficiency broadband rectifier with harmonic control for wireless power transfer and energy harvesting. IEEE Microwave and Wireless Components Letters, 32(10), 1231–1234. https://doi.org/10.1109/LMWC.2022.3174175

- Nguyen, D. A., Nam, H., & Seo, C. (2023). Design of compact Class-F high-efficiency shunt-diode rectifier with extended harmonic termination for wireless power transfer. *IEEE Microwave and Wireless Technology Letters*, 33(1), 78–81. https://doi.org/10.1109/LMWC.2022.3202760
- Shi, G., Shi, Z., Xia, Y., Jia, S., Xia, H., Shi, M., Sun, Y., Huang, Y., & Wang, B. (2024). A novel high-efficiency portable integrated system for synergistic harvesting of radio frequency and soil energy. *Energy Conversion and Management, 313*, Article 118594. https://doi.org/10.1016/j.enconman.2024.118594
- Wang, P. M., Bo, S. F., Ou, J. H., & Zhang, X. Y. (2025). High-efficiency wideband RF rectifier with enhanced dynamic power range based on impedance regulation network. *IEEE Microwave and Wireless Technology Letters*, *35*(3), 306–309. https://doi.org/10.1109/LMWT.2024.3523763
- Wu, P., Huang, S. Y., Zhou, W., Yu, W., Liu, Z., Chen, X., & Liu, C. (2019). Compact high-efficiency broadband rectifier with multi-stage-transmission-line matching. *IEEE Transactions on Circuits and Systems II:* Express Briefs, 66(8), 1316–1320. https://doi.org/10.1109/TCSII.2018.2886432
- Zhang, Z., Zhou, D., Gu, C., & Xuan, X. (2024). A broadband high-efficiency GaN transistor-based rectifier with variable phase shift. *IEEE Microwave and Wireless Technology Letters*, 34(10), 1198–1201. https://doi.org/10.1109/LMWT.2024.3450594